

# Determination of the source dwell position of an afterloading device with a detector array

F Breithuth<sup>1,2</sup>, H Schiefer<sup>1</sup>, M Arn<sup>1</sup>, S Peters<sup>1</sup>, W Seelentag<sup>1</sup>

<sup>1</sup>Department of Radiation-Oncology, Kantonsspital St.Gallen, Switzerland

<sup>2</sup>Department of Physics, Ludwig-Maximilians-University, Munich, Germany

## ABSTRACT

It was the aim to develop and test a measurement technique for the source position of an afterloading system using an electronic two-dimensional detector array (2D array). A "GammaMed plus IX" high dose rate afterloading device (Varian Medical Systems, Palo Alto, USA), and a Seven29 2D detector array (PTW Freiburg GmbH, Freiburg, Germany) have been used. A hollow needle has been connected to the afterloading device. Its outer diameter is 3.0 mm and its length about 220 mm. A 14 mm thick Perspex slab was fixed in a reproducible position on the 2D array. Above the 14<sup>th</sup> detector row, a groove was cut in the slab which accommodates the hollow needle in a fixed position relative to the 2D array. In order to define the position of the source, the signals of the detectors in the 14<sup>th</sup> detector row have been evaluated. A theoretical curve depending on the source position and strength has been fitted to the acquired detector signals. It has been shown that the mean reproducibility of the measurement technique - including the reproducibility of the source placement - was within 0.15 mm. This method can not only replace film measurements, it is also more exact and less time consuming.

**Keywords:** high dose rate brachytherapy, afterloading, dwell position, calibration, measurement, 2D detector array

**Disclosure:** The authors declare no conflicts of interest.

## 1. INTRODUCTION

Due to the local dose deposition next to the tumor, high-dose-rate brachytherapy (HDR) has been an established method in the fields of radiotherapy for a long time [1]. When the afterloading technique is used, the source is introduced in the patient via an applicator probe which is placed in the patient in advance of the irradiation. Depending on the tumor location, different methods and applicators are applied: Sharp hollow needles can be inserted directly into the tumor region and connected with the afterloading device, e.g. for cancers in the head and neck [2] or prostate [3]. Gynaecological tumors are treated by inserting cylindrical applicators with a suitable diameter in the vagina, or a tube in the cervix [4]. Intraluminal applicators are used for lung and esophagus [5] tumors.

Quality assurance procedures are described in a variety of regulations [6, 7]. From the physics point of view, among others the dwell time, dwell position and the strength of the radioactive source have to be included in the quality assurance procedures. The Swiss recommendations state that the accuracy of the source position has to be better than 2 mm. The calibration of the source position is usually performed with films. Different procedures have been suggested to regularly check the source positions: A transparent test phantom is monitored with a video camera, or a check ruler or a film are used [6].

In order to measure the position and the transit time of the radioactive source with a higher accuracy than with films, different measurement techniques have been developed. Rickey et al. [8] developed a quality assurance tool that combined a radiochromic film (Gafchromic films, Wayne, USA) with photodiode detectors. The accuracy of the dwell position was within 0.2 mm, and the dwell time was measured within about 1 ms. However, this method uses films and needs a processing machine and a film scanner. DeWerd et al. [9] designed a device that is able to measure the dwell position and time better than 1 mm and 1 s. They used a well ionization chamber which included a lead insert. The radiation of the source was focused with a collimator. The signal response of the ionisation chamber showed a strong depen-

\*ferdinand.breithuth@physik.uni-muenchen.de; phone +49 89 3000 3951; fax +49 89 30000 3569

dependency on the source position relative to the collimator hole. However, this method is time consuming and sophisticated to implement.

Until now, in St.Gallen the dwell position calibration has been performed based on film measurements (EDR2 ready pack films from Kodak, Rochester, USA). For this purpose, a hollow needle was connected to the afterloading device and fixed to the film surface. The needle tip was marked on the film with a pin prick. The source was placed by the afterloading device at different positions. The irradiated film was processed („Optimax 2010" from PROTEC medical systems, Johannesburg, South Africa) and manually evaluated. When a deviation of the measured position to the expected one was stated, the afterloading device was re-calibrated, and then the measurement was repeated. Despite the high effort, the accuracy of this procedure is limited. Due to the high costs and the time-consuming handling, it had been additionally decided to develop a filmless method, which should not exhibit these restrictions. It should also be using materials which are available in our clinic and in the many other radiotherapy institutions.

Two dimensional detector arrays (2D arrays) are widely used in radiotherapy for the quality assurance (QA) of different linear accelerator parameters and for dosimetric plan verifications [10, 11]. A 2D array based measurement technique to define the source position of an afterloading device is presented in this article.

## 2. MATERIAL AND METHODS

### 2.1 Material and measurement setup

The irradiations have been performed with a "GammaMed plus IX" high dose rate afterloading device (Varian Medical Systems, Palo Alto, USA). The source is an IR-192 rod with an active length of 3.5 mm and a diameter of 1.1 mm. A hollow metallic needle has been connected to the afterloader via the flexible guide tube. The measurements have been conducted with the detector array seven29 (PTW Freiburg GmbH, Freiburg, Germany) with a total of  $27 \times 27$  cubic detectors, arranged in a square grid with 10 mm spacing. The edge length of the cubic detectors is 5 mm. The 2D array acquisitions have been performed with the "MatrixScan" software (version 2.2., also from PTW Freiburg).

A 14 mm thick Perspex plate has been fixed on the detector array in a reproducible position. It contains at the upper surface a groove to house the metallic needle (inner diameter: 3.0 mm; usable length: about 220 mm). The inner diameter of the used catheter is 1.5 mm. The groove dimensions are 3.2 mm  $\times$  3.2 mm  $\times$  223.5 mm. By this means the source path in the needle is 20 mm above the detector centers in the 14<sup>th</sup> detector row. An additional 4.5 mm thick Perspex plate is placed on top: it fixes the needle in the groove and provides for sufficient backscatter. The needle end is about 8 cm distant from the central detector of the array. The signals of the detectors in the 14<sup>th</sup> row are evaluated to define the dwell position of the source. Further details of the plate construction are shown in Figure 1 and 2.

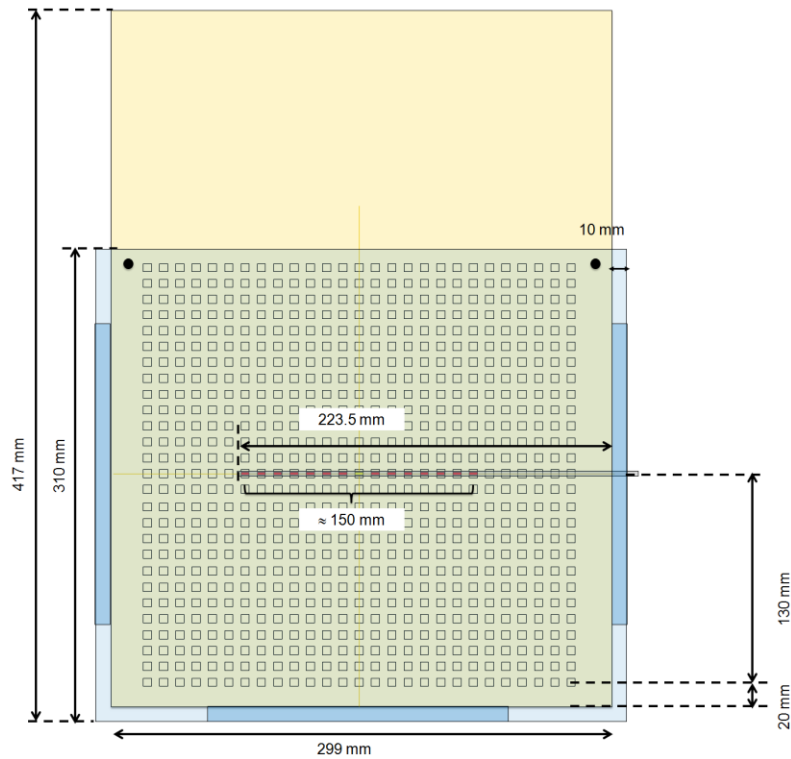


**Figure 1.** Top view on the 2D array (colored in transparent brown) and the Perspex plate (colored in transparent blue). The section of the source path, where measurements are supported without accuracy restrictions, is 15 cm long.

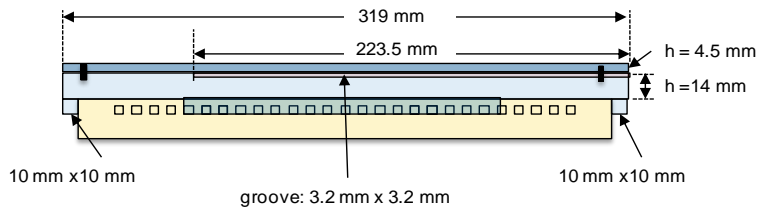


**Figure 2.** Front view on the 2D array and the Perspex plate (not to scale). The black squares symbolize the detector chambers.

For a sufficient accuracy of the calculated source position it is required, that the signals of the outer detectors in the 14<sup>th</sup> row drop down to less than 10% of the highest detector signal. With this restriction, 15 cm of the source path can be analyzed, including the furthest position at the needle tip.

The measurement setup is shown in Figure 3.

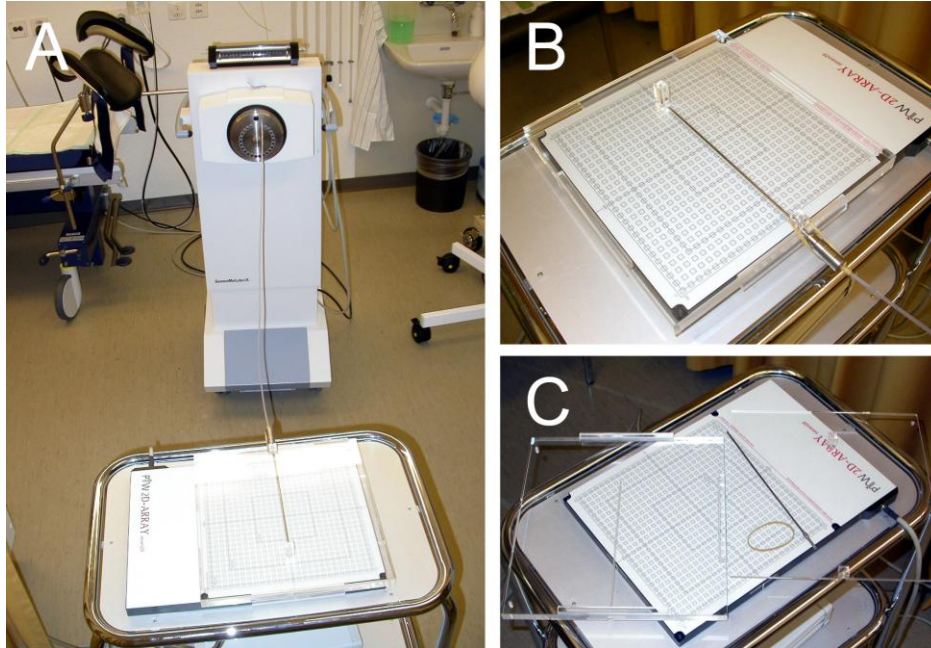


**Figure 3.** Measurement setup. A: It is made sure that the applicator connecting the needle with the afterloading device is in a stretched position. B: The needle is fixed in the needle guide with a rubber band. C: Components of the measurement setup. The plate fixing the needle in the needle guide is shown at the right.

### 2.2 Measurement method

The measurement procedure (shown in Figure 4) ensures that the source does not move during a measurement.

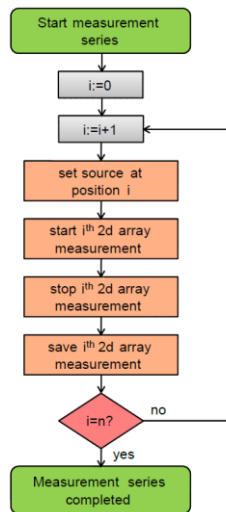


**Figure 4.** Measurement procedure for  $n$  single measurements at different source positions. Example: The source is 20 s at the  $i^{\text{th}}$  position. The user starts the array measurements, stops it after about 10 s and saves the measurement. Then, the source moves to the  $i+1^{\text{th}}$  position, and so on.

The source position in the coordinate system of the afterloading device is 130 cm at the applicator tip, and 129 cm, when the source is retracted by 1 cm. The 2D array is switched on at least 15 minutes before the measurement for stable readings.

### 2.3 User interface

Figure 5 shows the user interface of the Excel based measurement procedure.

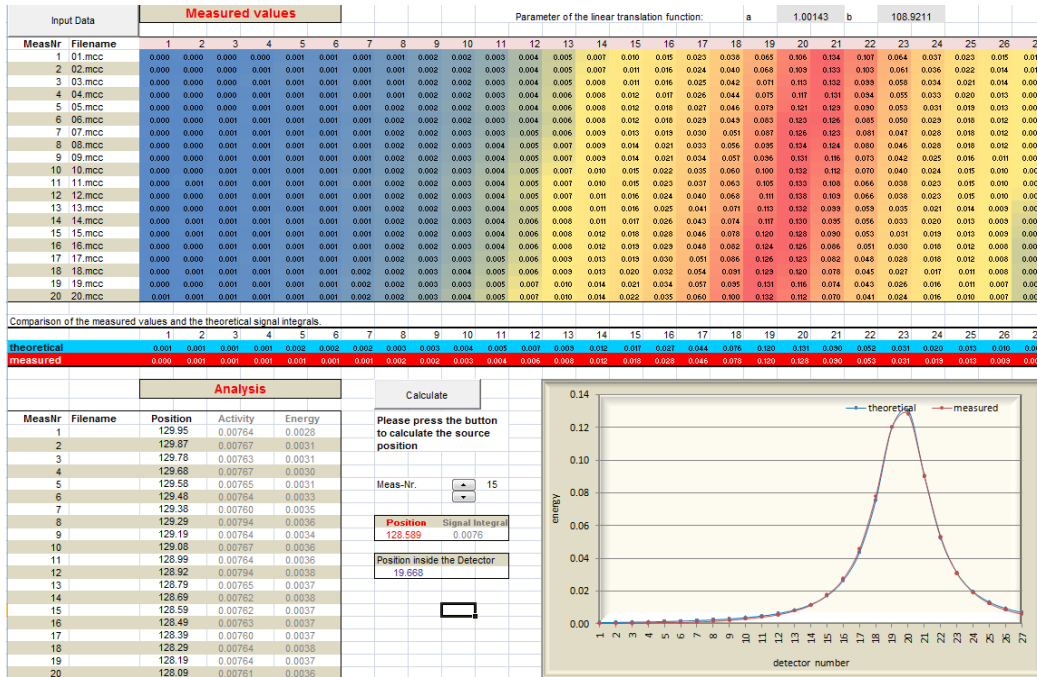


**Figure 5.** User interface of the measurement procedure. Twenty measurements, covering an "irradiated length" of 2 cm, are displayed in this example. The measurement values are encoded in red (high detector signal), yellow to blue (low detector signal).

The raw data are read by pressing the <Input Data> button. Twenty single measurements are evaluated in this example. The intensity of the detector signal is encoded with different colourings. In the first measurement, the source position is about above the detector nr. 21. In the following measurements 2 – 20, the source then moves in 1 mm steps to detector nr. 19. The evaluation is initialized by pressing the <Calculate> button. The source position, the "source strength" and the "energy" are calculated. Details to these quantities are described below.

### 2.4 Mathematical description of the evaluation method

As stated before, only the signals of the 14<sup>th</sup> detector row are evaluated. The evaluation principle is based on a comparison of the measured detector signals in the 14<sup>th</sup> row with the calculated signals in this row. The source is assumed to be a one-dimensional rod. The signal of the *i*<sup>th</sup> detector,  $D_c$ , is calculated as shown in equation (1):

$$D_c(i, p, S) = \int_{V, L} S \cdot d(x, y, z, l)^{-a} dx \cdot dy \cdot dz \cdot dl \quad (1)$$

The constant  $S$  is proportional to the source strength, named in the following as "source strength" for convenience.  $V$  is the detector volume;  $L$  is the source length. The source position is indicated as  $p$ .  $dx \cdot dy \cdot dz$  represents a differential volume element in the *i*<sup>th</sup> detector,  $dl$  is a differential element of the source.  $d$  describes the distance between the differential detector volume element and the differential source element. It is calculated as shown in equation (2):

$$d(x, y, z, l) = \sqrt{(x-l)^2 + y^2 + z^2} \quad (2)$$

$x$ ,  $y$ ,  $z$ , and  $l$  are the coordinates of the differential detector volumes and the source elements. The dwell position calculation is performed in the coordinate system of the 2D array: The  $y$  and  $z$  coordinates of the detector centres in the 14<sup>th</sup> row are 0. The  $x$  coordinate of the  $i^{\text{th}}$  detector is  $i$  cm.

The variable  $a$  in the exponent of equation (1) represents the distance dependence and should be equal to 2 if the distance square law would apply exactly. However, in order to take account of absorption processes, the exponent  $a$  was changed to  $a = 2.2$ . This value was determined experimentally by minimizing the difference between the calculated and measured values of multiple detector signals.

$D_c(i,p,S)$  is implemented in the code with the function *TheoreticalValue*.

The parameters  $p$  and  $S$  are varied iteratively in such a way that the calculated detector values  $D_c(i,p,S)$  coincide with the measured ones as close as possible. Let now  $D_m(i,p,S)$  be the measured value of the  $i^{\text{th}}$  detector for the position  $p$  and the source strength  $S$ . Then the objective function  $T(p,S)$  reads like:

$$T(p,S) = \sqrt{\sum (D_m(i,p,S) - D_c(i,p,S))^2} \quad (3)$$

The sum involves all detectors in the 14<sup>th</sup> detector row with detector signals larger than 10% of the maximum detector signal in the same detector row.  $T(p,S)$  describes the Pythagorean difference between  $D_m(i,p,S)$  and  $D_c(i,p,S)$  and is the square root of the error sum according to Gauss. When  $T(p,S)$  is at its minimum, the best values for  $p$  and  $S$  have been found, whereby  $p_s$  is the calculated dwell position of the source:

$$T(p_s, S_s) = \min(T(p,S)); \forall \{p,S\} \quad (4)$$

## 2.5 Numerical implementation

The program to calculate the source dwell positions has been written in Excel VBA (Visual Basic for Applications, Microsoft Excel Office 2007). In order to test the code behavior, some parameters in the code can be varied. The measurements and calculations which are presented in this article are performed with the parameter values given in the article. The same values are the defaults in the excel file, which can be downloaded from the journal's home page.

### 2.5.1 Initialization of the iteration process

Before the iteration starts, the detector values are read from the measurement files with the function *ReadInMeasuredValues*. This function also determines the maximal measured value, *MaxValue*, and the corresponding detector number. The number of the detector showing the maximal detector signal is used as the initial source position, *BestX*. The initial value for the source strength, *BestQ*, is estimated by the maximum signal in the detector row:

$$BestQ = 0.05736 MaxValue \quad (5)$$

*BestQ* defines the magnitude of the calculated detector signals. The factor 0.05736 has been determined by experience, and will depend on the individual detector array. Only detectors that exhibit at least 1/10 of the maximum measured signal are evaluated (The value of the lower limit, *UnderLimit*, is set to 0.1). A total dwell position interval of 15 cm can be evaluated when this restriction is considered. Following to equations (3) and (4), the main procedure *SourcePosition* then calculates iteratively the source position and the "source strength".

### 2.5.2 Calculation of the expected detector signals

Tests have shown that a division of the source by three differential sources and a division of the chamber volume by 3×3×3 differential volumes provides a good compromise between accuracy and calculation speed. The value of the constant which defines the fineness of the division, *ZS*, is therefore set to 3. By this means, the calculation sums over  $3^4 = 81$  differential volumes and sources per detector. The calculation is carried out in the function *TheoreticalValue*.

### 2.5.3 Calculation of the objective function

Following to equation (3), the function *CurrentEnergy* determines the value of the objective function. It depends on the actual source position and the source strength. In order to minimize the value of the objective function, the corresponding parameters are varied in the iteration.

### 2.5.4 Iterative determination of the source position

The source position is determined in the function *SourcePosition* by an alternating variation of the source strength and position variables and by calculating the associated objective function. When the variable with the smallest objective function is not at a border of the considered interval, the interval and the step size are downsized. The iteration stops when the step width for the position and source strength variables fall below the value of the variables *SmallestStepX* and *SmallestStepQ*. The function *SourcePosition* has three components. The first component contains the source position, the second one the source strength and the third component the value of the objective function. These parameters are shown in Figure 5 at the bottom left; indicated as “position”, “activity” and “energy”.

## 2.6 Calibration

As described above, the VBA code calculates the source position in the coordinate system of the array. This differs from the coordinate system of the afterloading system. In both coordinate systems the value of the dwell position decreases when the source is retracted in the treatment tube. As it will be shown in the results, the relation between the indicated dwell positions is linear:

$$x_{Afterloader} = a \cdot x_{Detector} + b \quad (6)$$

The values for  $a$  and  $b$  are determined in the course of the calibration. Since the detector distance is 1 cm, it can be expected that the value for  $a$  has to be close to +1. The measurements for the calibration were performed immediately after a calibration of the source position, which has been performed with film. Therefore it is assumed, that the source is positioned by the afterloading device correctly. The needle guiding plate and the needle were set up new before each measurement series. The parameters  $a$  and  $b$  were determined by a linear fit. Five measurements have been performed always at two subsequent days. The stated positions (set at the afterloading device) have been 130, 129..., 115 cm. The measurement time was 10 s. For the linear fit, the mean of ten measurements per source position has been used.

## 2.7 Tests of the measurement method

To test the measurement method, several measurements were performed. The flexible plastic guide tube, connecting the metallic needle to the afterloading device, was always carefully laid out straight, without actually pulling the needle. As shown by Palmer *et al.* [12], the effect of a bent catheter can cause deviations of several millimeters for the dwell positions.

### 2.7.1 Linearity of the measurement method

As an ideal situation, the correlation between the dwell position, which is selected by the afterloading device, and the measured position should be linear. Due to the symmetry of the measurement device and the evaluation algorithm, a non-linearity would give rise to the typical measurement characteristics shown in Figure 6 as an example.

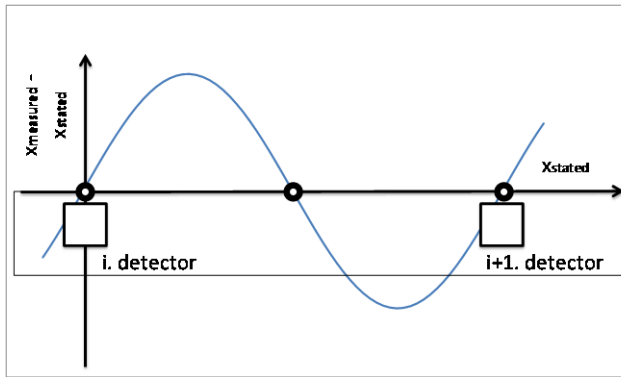


**Figure 6.** Typical non-linear behavior of the measurement system: It is assumed that the detectors of the 2D array have a perfect geometry (for instance identically constructed, detectors are equidistant arranged on a line and show identical sensitivities) and that the calibration is free from error. When the source is placed at points superior a detector or exactly in-between two adjacent detectors, no measurement error is present. These points act as benchmarks of the measurement technique. The deviation in the diagram has therefore to show point symmetry relative to these benchmarks. The drawing is not to scale.

The linearity of the measurement method was tested, whilst the source was placed by the afterloading device in arbitrary positions between the detectors. Two measurement series have been performed on different days. The needle guiding plate and the needle were set up new before each measurement series. The distance between adjacent dwell positions was 1 mm. The investigated source travel length was 5 cm. The dwell time was about 10 seconds for each position.

### 2.7.2 Influence of the source movement

The calibration of the measurement method has been performed with the procedure shown in Figure 3. It ensures that the source movement is not smearing the profile of the detector signals and in this way shifting the calculated source position.

To check the influence of the source movement on the registered source position, the procedure has been altered: The measurement interval included among the dwell time of the source at its designated position also the time when the source was moved to this position and when it was retracted in the afterloading device. The tests have been performed at the 123 cm position, where the source is nearly above the central detector of the array. The considered dwell times were 0.5, 1.0, 2.0, 5.0, 10.0, 15.0, 20.0, 30.0, 45.0 and 60.0 s. For each dwell time, 5 measurements were performed. The measurement setup was not changed during this measurement series.

### 2.7.3 Influence of the array switch on time

It is recommended by PTW that the 2D array should be switched on at minimum 5 minutes before a measurement is performed. It was tested if the measured dwell position depends on the switch on time of the detector array. For this purpose three measurement series have been acquired. Eight source positions per series have been investigated. The starting position was at 130 cm, and the step width was 2 cm. The dwell time was 10 s.

Two measurement series were performed with a switch on time smaller than 5 minutes. One series was done with a 15 minutes switch on time. The needle guiding plate and the needle were set up new before each measurement series.

## 3. RESULTS

### 3.1 Calibration

The result of the calibration is shown in Figure 7. The slope of the linear fit function is  $a = 1.0014$ , and  $b$  amounts to 108.92. The coefficient of determination,  $R$ , is 0.9999995. The mean standard deviation of the mean “measured source position” is 0.015 cm.

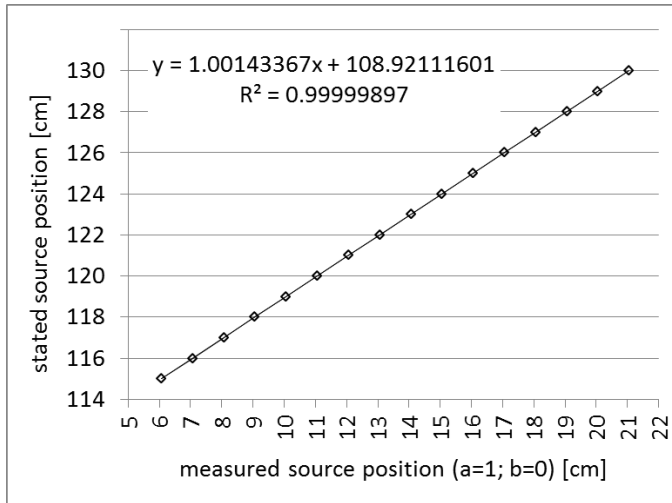


**Figure 7.** Determination of the transformation parameters *a* and *b*.

In order to check the calibration, the measurement files used to derive the *a* and *b* values are evaluated with the calibration presented above. Figure 8 shows the difference between the measured and the stated source positions.

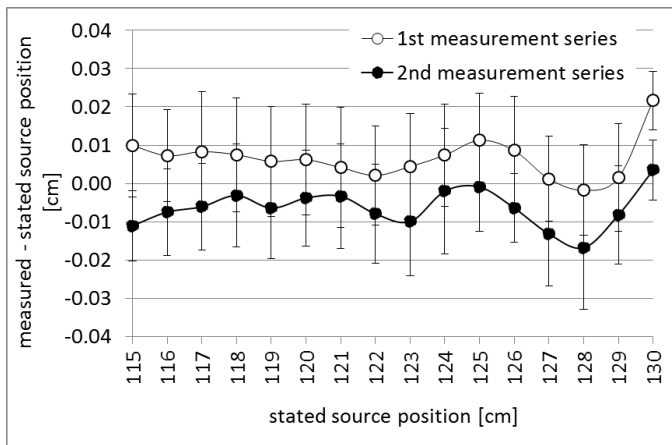


**Figure 8.** Evaluation of the measurements used for the calibration. Each measurement series is based on five single measurements for each source position.

The mean deviation of the stated to the measured source position of a single measurement is 0.014 cm. The mean absolute deviation of the considered measurement series is  $0.013 \pm 0.003$  cm. Since the measurement series and the calibration are not independent, this test is not really suitable to characterize systematic errors, however. The maximum deviation from the stated source position was 0.045 cm. 88.8% of the measured deviations were smaller than 0.020 cm.

### 3.2 Linearity of the measurement method

The evaluation of the linearity test is presented in Figure 9. The mean absolute deviation of a single measurement from the stated position is  $0.012 \pm 0.008$  cm. The mean absolute difference between the series is  $0.022 \pm 0.004$  cm.

The data points have been grouped with respect to the relative position to the adjacent detectors. The group indicated with “x.0” includes the measurements at the source positions 130.0, 129.0 ... 125.0 cm, the group indicated with “x.1” includes the measurements at the source positions 129.1, 128.1 ... 125.1 cm, and so on up to “x.9”. The mean deviation is always in the [0.010, 0.016] interval. The interval width is therefore about 0.006 cm. The groups “x.0” and “x.1” show larger deviation. But this is valid also for the corresponding standard deviations which qualifies this statement.

The *b* value of the linear calibration function is 108.92. When a non-linearity would be present, the “x.9” and the “x.4” group should present the smallest deviations. This does certainly not apply for the “x.9” group. Independent of this statement, a possibly present deviation from a linear measurement behavior affects the measurement accuracy by less than the half of the interval width, which is 0.003 cm.

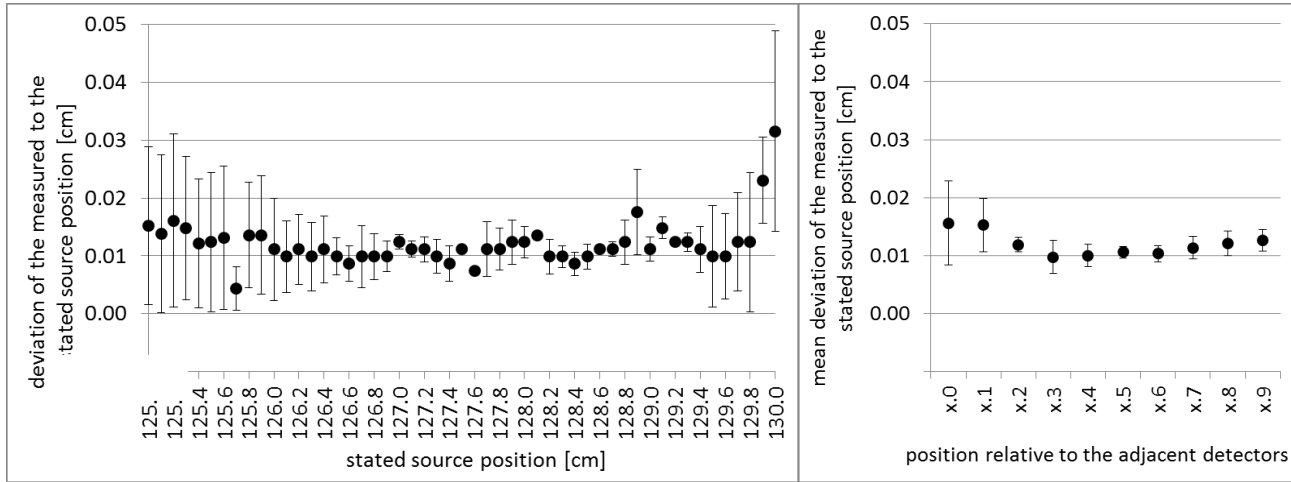


**Figure 9.** Left diagram: Mean deviation of the measured to the stated source position. Right diagram: Mean deviation of the grouped source positions.

**3.3 Influence of the source movement**

Figure 10 shows the mean detector signals for five measurements and dwell times from 0.5 s to 60 s. The detector values are normalized to the maximum signal of the corresponding measurement. The standard deviation per measurement position is in the mean 0.5% of the maximum detector signal and therefore not indicated in Figure 10. The source enters from the left side (detector 1) of the diagram and moves initially to the position at the needle tip which corresponds to 130 cm in the coordinate system of the afterloading device. This position lies next to the detector number 21, as incorporated in the calibration and seen also in Figure 4. By moving towards the foremost position in advance of an irradiation series, the afterloading device checks if the applicator assembly is of the required total length, and if it is fixed properly to the afterloading device.

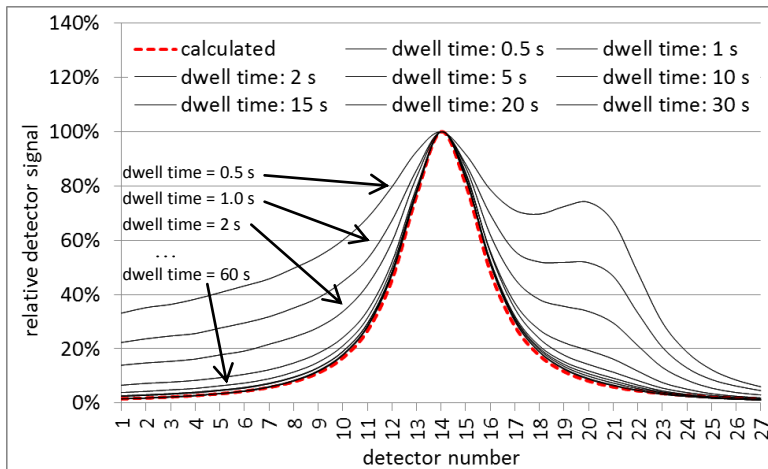


**Figure 10.** Dependency of the signal slope on the dwell time when the source movement is included in the measurement time interval. Each curve is based on five measurements.

For small dwell times, the signal originating from the reversal point of movement is in a comparable order as the signal generated at the provided dwell position. It would be obvious that the registered dwell position is translated by this effect. When the dwell time is elongated, the normalized shape of the detector signals approximates asymptotically to

the “calculated” shape of the detector signals. As stated above, the “calculated” shape is based on an acquisition which does not include source movements.

Figure 11 shows the measured and corresponding calculated detector signals when the dwell time is 0.5 s. The deviation of the measured to the calculated detector signals is caused on the left side of the signal peak when the source is moved from the afterloading device to the provided position, and later back to the afterloading device. The deviation on the right side of the peak is caused by the movement to the needle tip and then back to the provided source position.

Despite the signal contributions of the moving source, the peak of the calculated signal shape, which is based on the measured asymmetrical detector signals, is surprisingly close to the peak of the measured signal profile.

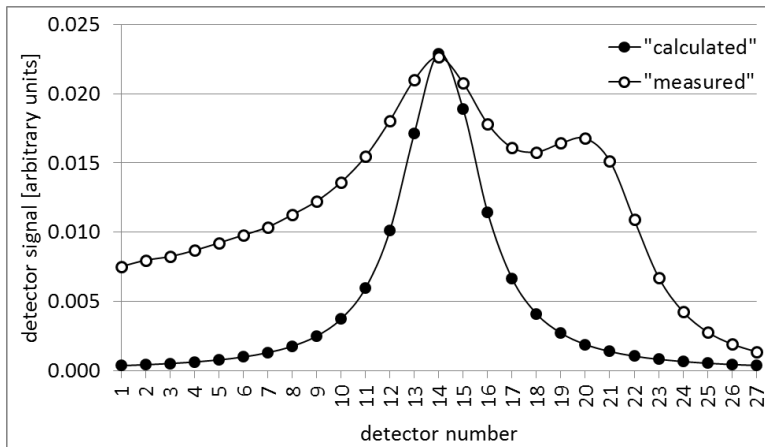


**Figure 11.** Measured detector signals for a 0.5 s dwell time, and corresponding calculated signals. Although the shapes of the profiles differ markedly, the peaks of the curves lie at very similar positions. It must be expected that this behaviour does not apply when the source is placed away from the centre of the detector row when one shoulder of the signal shape is cut.

The calculated source positions for the considered dwell times are presented in Figure 12. The longer the dwell time, the smaller is the difference between the stated and the calculated source position.

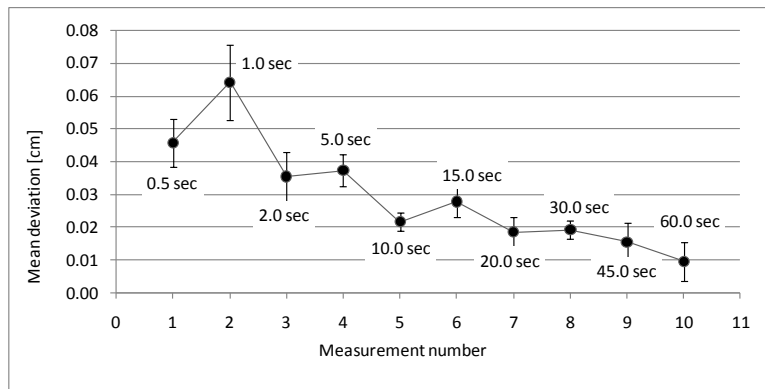


**Figure 12.** Mean deviation of the stated to the calculated source position for different dwell times, when the source movement is included in the measurement interval. The deviation goes asymptotically towards zero when the dwell time is increased.

When the dwell time is 10 s, the measured and stated source positions agree within about 0.02 cm.

### 3.4 Influence of the array switch on time

For switch on times smaller than five minutes, the deviation between the measured and the stated source position is in a wider range than when the switch on time is 15 minutes (table 1). The mean deviation from the theoretical (stated by the afterloading device) source positions is  $-0.036 \text{ cm} \pm 0.010 \text{ cm}$  and  $0.046 \text{ cm} \pm 0.009 \text{ cm}$ , when the switch on time is less than 5 min, it is  $0.008 \text{ cm} \pm 0.007 \text{ cm}$ , when it is more than 15 min. The mean absolute difference between the series is  $0.083 \pm 0.004 \text{ cm}$ , which is large when compared with other results presented here. The deviations are nevertheless clearly smaller than 2 mm, as required in the Swiss recommendations [6].

| Switch on time < 5 min |        | Switch on time<br>15min | Theoretical<br>position |
|------------------------|--------|-------------------------|-------------------------|
| 129.94                 | 130.03 | 129.98                  | 130.00                  |
| 127.97                 | 128.05 | 128.01                  | 128.00                  |
| 125.97                 | 126.05 | 126.00                  | 126.00                  |
| 123.96                 | 124.04 | 124.00                  | 124.00                  |
| 121.97                 | 122.05 | 122.01                  | 122.00                  |
| 119.97                 | 120.05 | 120.01                  | 120.00                  |
| 117.96                 | 118.04 | 118.00                  | 118.00                  |
| 115.97                 | 116.06 | 116.01                  | 116.00                  |

**Table 1.** Source positions [cm] depending on the switch on time of the 2D array. The measurement itself lasted about three minutes. The accuracy is better after a switch on time of 15 minutes (and more).

#### 4. DISCUSSION

A 2D array based method to measure the dwell position of an afterloading device in a fast and accurate way has been presented. The accuracy was checked with different tests: The measurement method shows a strict linear correlation between the source position stated by the afterloading device and the measured source position. The mean deviation between the stated and the measured source position is 0.015 cm, independent on the position of the source relative to the adjacent detectors. It has been shown that the accuracy is not essentially reduced when the needle guiding plate is remounted on the 2D array before a measurement is performed.

Different details have to be considered when highest possible measurement accuracy should be achieved: In order that the guide wire is not coiled or wreathed, the catheter has to be arranged in a stretched position [12]. It is recommended to apply the measurement procedure which is shown in Figure 3. In this way the movement of the source, which would smear the profile shape, is excluded from the measurement interval. This is substantial especially for short acquisition times and when the source is placed outside the central area of the detector. It is recommended switching on the 2D array at minimum 15 minutes before measurements are performed.

But, independent on these recommendations, the measurement method fulfills the requirements which are set for instance in the Swiss recommendations [6].

#### 5. CONCLUSION

When a 2D array is available, the presented measurement method can be introduced with little effort. It is time effective and accurate.

In the current version it is not supported to check also the dwell time and the source strength. The procedure can be in principle expanded as follows, however:

*Measurement of the source strength:* The Perspex plate shown in Figure 1 and 2 is provided with a mechanism to fix a reference source with long half-life in a reproducible position, preferably in the centre of the 2D array. An acquisition is performed for one minute. Subsequently, a measurement with the afterloading source placed in the central area of the detector is performed for one minute, applying the procedure described in Figure 3. The “source strength”, as introduced in equation (1), is evaluated for both measurements;  $S_R$  and  $S_A$ . (Alternatively, the sum of the detector signals can be used.) The ratio of these quantities,  $S_A:S_R$ , is independent on systematic variations as for instance temperature and air pressure. When the decay of the reference source is taken into account,  $S_A:S_R$  is proportional to the strength of the afterloader source. The proportionality factor is defined by a cross calibration, when the conventional measurement technique is used to define the source activity.

*Measurement of the dwell time:* The dwell times provided by the afterloading system,  $t$ , do not include the time of source movement to the first source dwell position. The corresponding interfering signal,  $S_M$ , appears as a constant offset to the integral signal,  $S_A$ . Therefore, equation (7) is valid:

$$S_A = c \cdot t + S_M \quad (7)$$

When two single dwell position measurements with different dwell times,  $t_1$ ,  $t_2 = 2 \times t_1$ , are performed,  $S_M$  and the constant  $c$  can be determined. Figure 4 implies that the  $S_M$  contribution corresponds to the signal of a 0.5 to 1 s long dwell time.  $t_1$ , specified in the afterloading software, is ideally 60 s. It is checked manually with a chronograph and confirms the absolute time value. This procedure is sufficient to check the timer absolute accuracy within 2%, as prescribed by the Swiss recommendations [6]. The linearity is checked with different dwell times, for instance 20, 10, 5, 2 and 1 s.

## REFERENCES

- [1] Fleming, P., Nisar S., Neblett D. et al. Description of an afterloading <sup>192</sup>Ir interstitial-intracavitary technique in the treatment of carcinoma of the vagina. *Obstetrics & Gynecology* 55(4), 403-531 (1980).
- [2] Glatzel M., Büntzel J., Schröder D. et al. High-dose-rate brachytherapy in the treatment of recurrent and residual head and neck cancer. *Laryngoscope* 112, 1366-1371 (2002).
- [3] Hoskin P. High dose rate brachytherapy for prostate cancer. *Cancer Radiother.* 12(6-7), 512-514 (2008),
- [4] Stitt J. A. High dose rate brachytherapy in the treatment of cervical carcinoma. *Hematol. Oncol. Clin. North Am.* 13(3), 585-593 (1999).
- [5] López Carrizosa M.C., Samper Ots P.M., Rodríguez Pérez A. et al. High dose rate brachytherapy (HDR-BT) in locally advanced oesophagus cancer. Clinical response and survival related to biological equivalent dose (BED). *Clin. Transl. Oncol.* 9(6), 385-391(2007).
- [6] Schweizerische Gesellschaft für Strahlenbiologie und Medizinische Physik (SGSMP). Dosimetry and Quality Assurance in High Dose Rate Brachytherapy with Iridium-192. Recommendations No. 13, ISBN 3 908 125 36-7 (2005)  
On the internet: <http://sgsmp.ch/r13hdr-e.pdf>.
- [7] Deutsche Gesellschaft für Medizinische Physik e.V. (DGMP). Leitlinie zu Medizinphysikalischen Aspekten der intravaskulären Brachytherapie. ISBN 3-925218-70-X, (2001)  
On the internet: <http://www.dgmp.de/oeffentlichkeitsarbeit/papiere/Bericht16.pdf>.
- [8] Rickey D.W., Sasaki D., Bews J. A quality assurance tool for high dose rate brachytherapy. *Med. Phys.* 37(6), 2525-32 (2010).
- [9] DeWerd L.A., Jursinic P., Kitchen R. et al. Quality assurance tool for high dose rate brachytherapy. *Med. Phys.* 22(4), 435-440 (1995).
- [10] Spezi E., Angelini A.L., Romani F. et al. Characterization of a 2D ion chamber array for the verification of radiotherapy treatments. *Phys. Med. Biol.* 50(7), 3361 (2005).
- [11] Poppe B., Blechschmidt A., Djouguela A. et al. Two-dimensional ionization chamber arrays for IMRT plan verification. *Med. Phys.* 33(4), 1005-1015 (2006).
- [12] Palmer A. and Mzenda B. Performance assessment of the BEBIG MultiSource<sup>®</sup> high dose rate brachytherapy treatment unit. *Phys. Med. Biol.* 54(11), 7417-7434 (2009).